AFGL-TR-78—0071
INSTRUMENTATION PAPERS, NO. 266

LEVEL

# The Topside Ionosphere Plasma Monitor (SSIE) for the Block 5D/Flight 2 DMSP Satellite

M. SMIDDY
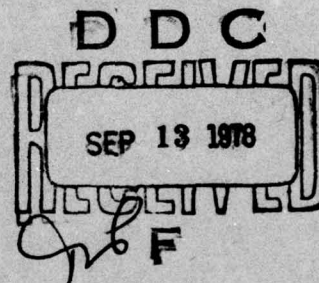R. C. SAGALYN
W. P. SULLIVAN
P. J. L. WILDMAN
P. ANDERSON
F. RICH

DDC

RECEIVED
SEP 13 1978
F

22 MARCH 1978

SPACE DIVISION      PROJECT 2311
## AIR FORCE GEOPHYSICS LABORATORY
HANSCOM AFB, MASSACHUSETTS 01731

## AIR FORCE SYSTEMS COMMAND, USAF

78  14  08  264
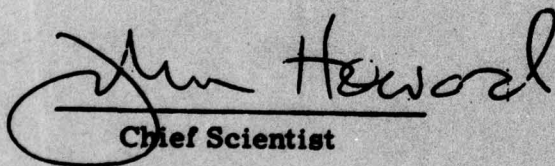
| REPORT DOCUMENTATION PAGE | READ INSTRUCTIONS BEFORE COMPLETING FORM |
|---|---|

| 1. REPORT NUMBER | 2. GOVT ACCESSION NO. | 3. RECIPIENT'S CATALOG NUMBER |
|---|---|---|
| AFGL-TR-78-0071 $AFGL-IP-266$ | | |

| 4. TITLE (and Subtitle) | 5. TYPE OF REPORT & PERIOD COVERED |
|---|---|
| THE TOPSIDE IONOSPHERE PLASMA MONITOR (SSIE) FOR THE BLOCK 5D/FLIGHT 2 DMSP SATELLITE. | Scientific. Interim. |
| | 6. PERFORMING ORG. REPORT NUMBER |
| | IP No. 266 |

| 7. AUTHOR(s) | 8. CONTRACT OR GRANT NUMBER(s) |
|---|---|
| M. Smiddy, P.J.L. Wildman R.C. Sagalyn, P. Anderson W.P. Sullivan, F. Rich* | |

| 9. PERFORMING ORGANIZATION NAME AND ADDRESS | 10. PROGRAM ELEMENT, PROJECT, TASK AREA & WORK UNIT NUMBERS |
|---|---|
| Air Force Geophysics Laboratory (PHR) Hanscom Air Force Base Massachusetts 01731 | 61102F 2311G205 G2 |

| 11. CONTROLLING OFFICE NAME AND ADDRESS | 12. REPORT DATE |
|---|---|
| Air Force Geophysics Laboratory (PHR) Hanscom Air Force Base Massachusetts 01731 | 22 March 78 |
| | 13. NUMBER OF PAGES |
| | 36 |

| 14. MONITORING AGENCY NAME & ADDRESS(if different from Controlling Office) | 15. SECURITY CLASS. (of this report) |
|---|---|
| | Unclassified |
| | 15a. DECLASSIFICATION/DOWNGRADING SCHEDULE |

16. DISTRIBUTION STATEMENT (of this Report)

Approved for public release; distribution unlimited. 39 p.

17. DISTRIBUTION STATEMENT (of the abstract entered in Block 20, if different from Report)

Instrumentation papers,

18. SUPPLEMENTARY NOTES

*Regis College, Weston, MA 02193

19. KEY WORDS (Continue on reverse side if necessary and identify by block number)

Ionosphere
Topside ionosphere
Thermal plasma
Plasma scale height

Electron sensor theory
Ion sensor theory

20. ABSTRACT (Continue on reverse side if necessary and identify by block number)

The Topside Ionosphere Plasma Monitor (SSIE) is an operational system flown on the Block 5D F2 DMSP Satellite for transmission of continuous data on the state of the topside ionosphere. The instrument consists of separate electron and ion sensors mounted on a 2.5-ft boom deployed after spacecraft attitude has been stabilized in orbit. This report describes the two sensors, associated electronics, and their operational timelines. The theoretical basis → next page

DD FORM 1473 EDITION OF 1 NOV 65 IS OBSOLETE
1 JAN 73

78 14 08 264

409 578

20. Abstract (Continued)

is given for the measurement of a number of plasma parameters: electron temperature and density, ion density, average ion temperature and mean ion mass (for one or two ion species), spacecraft potential, and plasma scale height.

## Contents

## Illustrations

Tables

# The Topside Ionosphere Plasma Monitor (SSIE) for the Block 5D/Flight 2 DMSP Satellite

## 1. INTRODUCTION

This report describes the Topside Ionosphere Plasma Monitor flown on the Block 5D/Flight 2 Satellite of the USAF Defense Meteorological Satellite Program (DMSP). The plasma monitor, designated as Special Sensor Ion/Electron (SSIE), consists of an electron sensor and an ion sensor mounted on a boom from the DMSP satellite as shown in Figure 1. The electron sensor measures the ambient electron density and temperature and the electrostatic potential of the vehicle with respect to the ambient plasma. The ion sensor measures the densities of the major ion species present, the average ion temperature, the average ion mass, and the vehicle potential. The plasma scale height at the satellite is determined with the use of both instruments. From the continuous readout of data from the plasma monitor, the plasma scale height and density are determined as a function of time, and plasma irregularity spectra can be calculated. The vehicle potentials and plasma densities obtained independently from the ion and electron sensors are compared as a check of instrument performance and of data reduction procedures.

The electron sensor of the SSIE system is a spherical Langmuir probe. The electron sensor, together with its electronics, is shown schematically in Figure 2. The flight hardware and the electron data analysis procedure are described in Section 2. The ion sensor of the SSIE system is a planar electrostatic particle

---

trap.   The ion sensor and its electronics are shown schematically in Figure 3.
The flight hardware and the ion data analysis procedure are described in Section 3,
the method of determining the plasma scale height, in Section 4, and the SSIE
telemetry allocations and electronics, in Section 5.   The time sequence of events,
bias, sweep, and internal calibrations for both sensors are given in Table 1.



**ELECTRON SENSOR**

12"

**ION SENSOR**

19"

**SOLAR CELLS**

SPACECRAFT VELOCITY

1 + X AXIS POINTS VERTICALLY TO
   EARTH AT ALL TIMES

2 VELOCITY VECTOR PARALLEL WITH
   -Y AXIS

3 NORMAL TO ION SENSOR PARALLEL
   WITH -Y AXIS

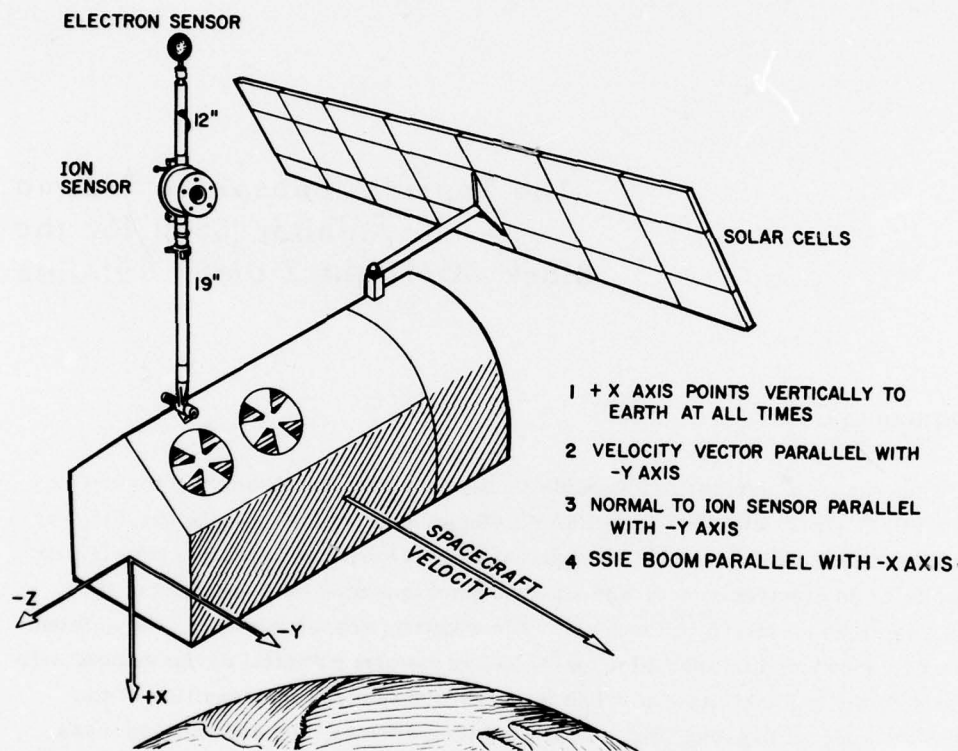4 SSIE BOOM PARALLEL WITH -X AXIS

-Z

-Y

+X

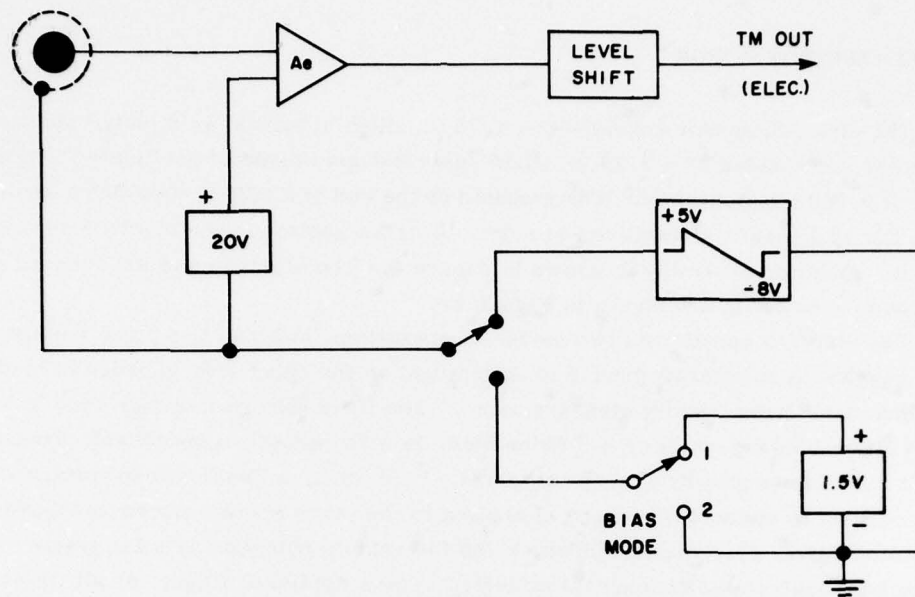Figure 1.   F2 Spacecraft Showing Location of SSIE Sensors (not to scale)

6

Figure 2. Block Diagram of SSIE Electron Experiment
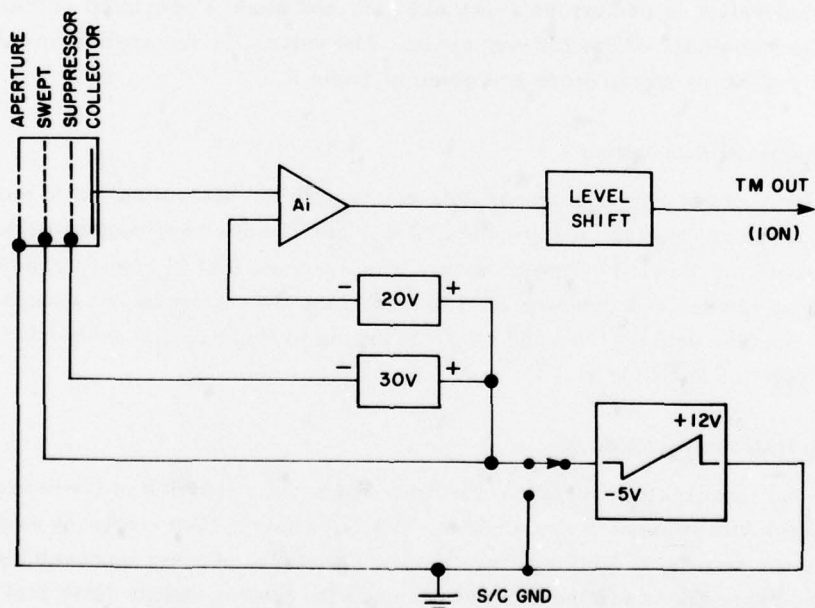


Figure 3. Block Diagram of SSIE Ion Experiment

7

## 2. THE ELECTRON SENSOR

The electron sensor consists of a 1.75 in. diam spherical gold plated aluminum collector surrounded by a 2.25 in. diam spherical grid made of gold plated tungsten wire of 0.800 transparency. It is mounted at the end of a 2.5-ft rigid boom deployed after the spacecraft is stabilized in orbit. A cross section of the electron sensor with its mounting assembly is shown in Figure 4. The electron and ion sensors attached to the boom are shown in Figure 5.

The electron sensor has two modes of operation: In Mode 1, a fixed voltage with respect to spacecraft ground is maintained on the outer grid in order to obtain continuous electron density measurements. The fixed voltage is either +1.5 V (Bias Mode 1 in Figure 2) or 0 V (Bias Mode 2) with respect to spacecraft ground, and it may be changed by ground command. In Mode 2, a linear sweep voltage with respect to spacecraft ground is applied to the outer grid as shown in Figure 2. This mode gives electron temperature and the vehicle potential by a Langmuir probe type analysis of the current collected versus applied voltage. At all times, the voltage on the collector is +20 V with respect to the outer grid to ensure that all electrons passing through the outer grid will be collected. Mode 1 and Mode 2 operations of the electron sensor are automatically alternated by the SSIE Time Sequencer as described in Table 1 and Section 5.1. One Mode 2 sweep operation of 10-sec duration is performed every 128 sec, and Mode 1 operation is maintained during the remainder of the 128-sec cycle. The values for the applied voltages during the electron sweep mode are given in Table 2.

### 2.1 Electron Sensor Data Analysis

Analysis of the electron sensor data starts with the determination of the electron temperature $T_e$, the vehicle potential $\phi_s$, and the electron number density $N_e$ from analysis of the Mode 2 sweep data. It is assumed that $T_e$ and $\phi_s$ are constant for the next 128 sec and they are used to determine the instantaneous values of the ambient electron density from the current flowing to the electron sensor in the fixed voltage mode (Mode 1).

### 2.2 Sweep Mode Analysis (Mode 2)

The current ($I_e$) to a spherical electron sensor is a function of the sensor potential ($\phi$) with respect to the plasma. If $\phi$ is positive, then electrons are accelerated to the sensor; if $\phi$ is negative, they are retarded as they approach the sensor. The expressions for the current reaching the sensor and its first derivative are given here, assuming a Maxwellian distribution function for the ambient electron population for a retarding potential ($\phi < 0$):

8
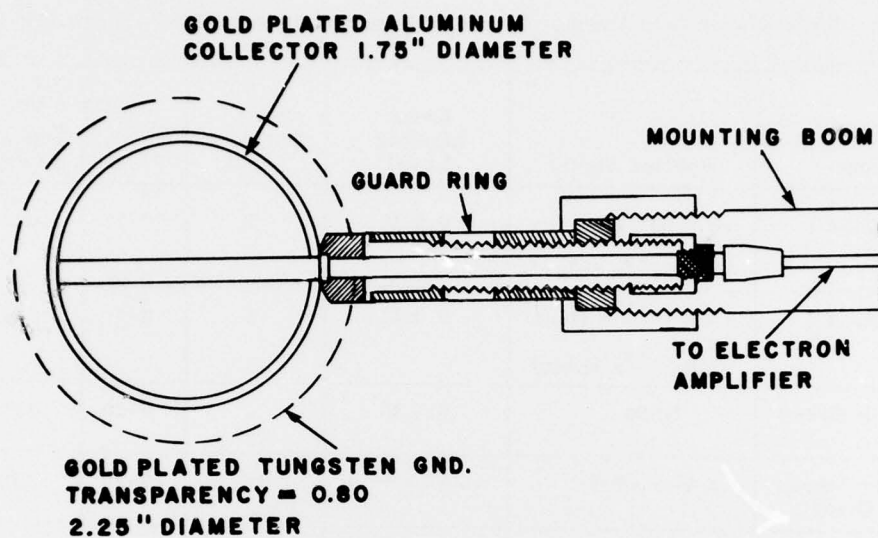
Figure 4.  Cross Section of SSIE Electron Sensor
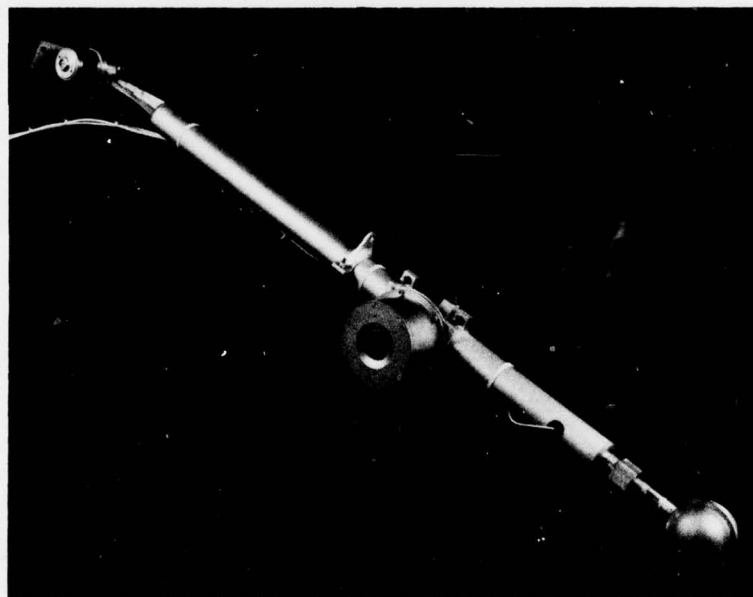


Figure 5.  SSIE Experiment 2.5-ft Rigid Boom Showing Location of Sensors

9

Table 1. Time Sequence of Events, Bias and Sweep Voltages, DMSP, Block 5D, F2

| Event | Applied Signal | Event Monitor Level | Duration (sec) | Time (sec) First | Time (sec) Repeats Every |
|---|---|---|---|---|---|
| Calibration 1 | $+5 \times 10^{-8}$a (Ion) $-1 \times 10^{-6}$a (Elec) | 0.2 V | 2 | 0-2 | 1024 |
| Calibration 2 | $+5 \times 10^{-11}$a (Ion) $-1 \times 10^{-9}$a (Elec) | 0.4 V | 2 | 2-4 | 1024 |
| Electron Sweep Flag | None | 0.6 V | 2 | 8-10 | 128 |
| Electron Sweep (Outer Grid) | +5 V → -8 V | +5 V → +1 V | 10 | 10-20 | 128 |
| Ion Sweep Flag | None | 0.8 V | 2 | 24-26 | 128 |
| Ion Sweep (Outer Grid) | -5 V → +12 V | +1 V → +5 V | 12 | 26-38 | 128 |

| Bias Mode | Resting Bias Electron Density Grid | Mode Monitor (Analog No. 49) |
|---|---|---|
| 1 | 1.5 V | 3.5 V |
| 2 | 0 V | 1.5 V |

$$I_e = Ae \, \alpha N_e \, a \, \exp{(-x^2)}/2\sqrt{\pi} \tag{1}$$

$$\partial I_e / \partial \phi_p = -Ae^2 \, \alpha N_e \, a \, \exp{(-x^2)}/2 \, kT_e \sqrt{\pi} \tag{2}$$

For an accelerating potential ($\phi > 0$),

$$I_e = Ae \, \alpha N_e \, a \, (1 - x^2)/2\sqrt{\pi} \tag{3}$$

$$\partial I_e / \partial \phi_p = -Ae^2 \, \alpha N_e \, a/2 \, kT_e \sqrt{\pi} \tag{4}$$

where

$$x^2 = a^{-2} \, (2 \, e \, \phi/m_e) \tag{5}$$

10

$\phi$  = potential of sensor with respect to plasma = $\phi_s + \phi_p$ (volts)

$\phi_s$  = potential of vehicle with respect to plasma (volts)

$\phi_p$  = potential of sensor with respect to vehicle (volts)

A  = surface area of sensor (m$^2$) = $4\pi r^2$, where r is sensor radius = 0.028575 m

e  = electron charge = $1.602 \times 10^{-19}$ coulomb

$\alpha$  = sensor transparency = 0.800

$N_e$  = ambient electron density (m$^{-3}$)

$m_e$  = electron mass = $9.1085 \times 10^{-31}$ kg

a  = $(2\,kT_e/m_e)^{1/2}$ = most probable electron speed (m sec$^{-1}$)

$T_e$  = electron temperature ($^{\circ}$K)

k  = Boltzmann constant = $1.38054 \times 10^{-23}$ joule/$^{\circ}$K

To obtain $T_e$, we make use of the linear relation between Log $(-I_e)$ and $\phi_p$ in the retarding portion of the $I_e$ vs $\phi$ curve. (We will denote $\text{Log}_{10}$ by "Log" and use 'ln' for natural logs.) By substituting

$$\partial \text{Log}\,(-I_e)/\partial \phi_p = (\ln(10))^{-1}\,\partial(-I_e)/I_e\,\partial\phi_p \tag{6}$$

and Eq. (1) into Eq. (2), we obtain

$$\partial\,\text{Log}\,(-I_e)/\partial\phi_p = e/k\,T_e\,\ln(10) \tag{7}$$

Thus

$$T_e = \frac{5040}{S}\,^{\circ}\text{K} \tag{8}$$

where S is the slope of the semi-log plot of $I_e$ vs $\phi_p$.

In Figure 6, Log $(-I_e)$ and its derivative are plotted as a function of $\phi_p$. The point $\phi_0$ indicated on the curve is the point at which the probe is at plasma potential ($\phi = 0$) and it is the intersection of the exponential (retarding) and linear (accelerating) portions of the $I_e$ vs $\phi_p$ curve. From this point, we obtain the value of vehicle potential $\phi_s$ with respect to the plasma

$$\phi_s = -\phi_0 \tag{9}$$

11
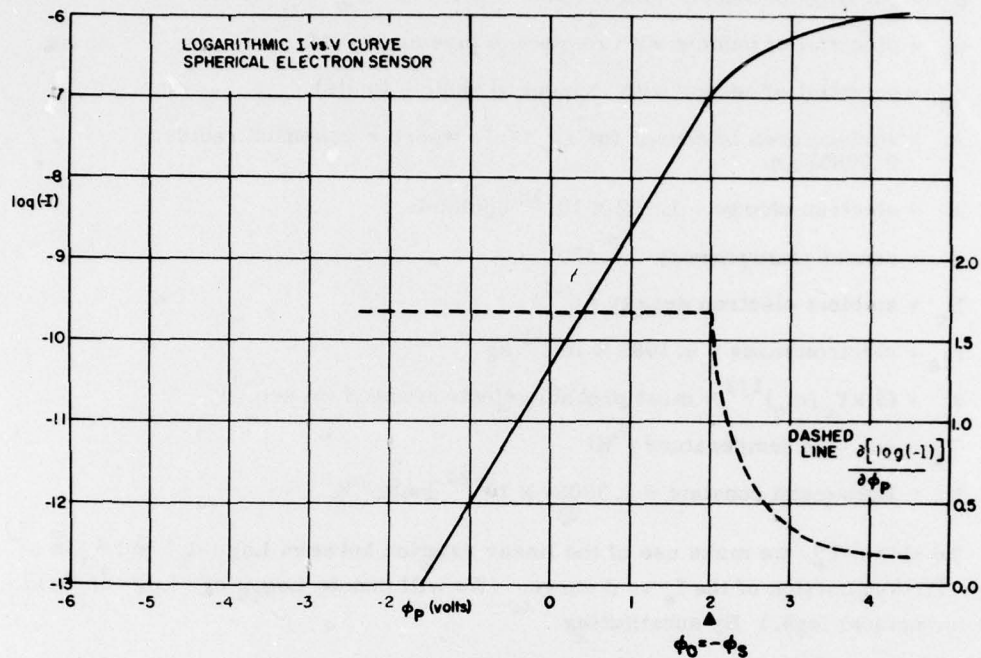
Figure 6. Electron Sensor Theory: $\text{Log}_{10}(I)$ vs $\phi_p$ and First Derivative

Using the current $I_o$ measured when the probe is at plasma potential ($\phi = 0$), one calculates the value of the ambient electron density $N_e$ at the time of the sweep from Eq. (1).

$$N_e(t_o) = 2\sqrt{\pi}\, I_o / Ae\, \alpha\, a \quad . \tag{10}$$

Equations (1) through (4) are based on the assumption that $|e\phi| \lesssim kT$. In fact, the range of the swept voltages may exceed the range of voltage where this assumption is valid. In the accelerating potential region, the finite Debye length (length that the probe's electrostatic field can reach into the plasma) causes the current to the probe to be limited. The slope of the $(-I_e)$ vs $\phi$ curve is less than that given by Eq. (4) when $\phi - \phi_o \lesssim 1.0$ V. In the retarding potential region, the measured current to the probe can be significantly more than the value given by Eq. (1) when $\phi - \phi_o \lesssim -2$ V, due to high energy components of the ambient plasma, secondary and photoelectrons from the grid surfaces, and the sensitivity limits of the instrument electronics. The data analysis procedure in Section 2.4 is designed to avoid the ranges of the potential for which the foregoing assumption $|e\phi| \lesssim kT$ is invalid.

12

## 2.3 Fixed Voltage Mode Analysis (Mode 1)

Once $N_e$ and $T_e$ have been determined from analysis of the sweep mode data, one can proceed to derive $N_e$ at all other times if it is assumed that $T_e$ and $\phi_s$ do not change during the 128-sec interval between sweeps. During this interval, the 0 V or +1.5 V resting bias is applied to the grid of the electron sensor. If we designate this resting bias by R volts, then the electron density at any time t during the fixed voltage Mode 1 operation is

$$N_e(t) = I_e(t) \, N_e(t_o)/I_e(R) \tag{11}$$

where $I_e(t)$ is the sensor current at time t, $I_e(R)$ is the sensor current during the sweep when $\phi_p = R$ volts, and $N_e(t_o)$ the electron density derived from the sensor current with the probe at plasma potential in Eq. (10).

## 2.4 Electron Data Reduction Procedure

The steps followed for the analysis of the electron data are:

1. Take the Mode 2 measured current $I_e$ as a function of $\phi_p$. From the start of the sweep in time ($\phi_p = +5$ V), fit a straight line to 3 data points to determine the slope, and then move the fitting process through the entire sweep, one point at a time. (Measured currents corresponding to the maximum voltage on the telemetry channel are disregarded because the true current is out of range.) We find the potential $\phi_{LIN}$ at which the absolute value for the slope of a 3-point fit centered on $\phi_{LIN}$ is a maximum. If two or more fits give the same maximum, choose the fit for the most negative value of $\phi_{LIN}$.

2. Take Log $(-I_e)$ as a function of $\phi_p$ and do same 3-point fit as in step 1 to find the maximum absolute value of the slope. This time if two or more fits give equal maximum slopes, take the <u>first</u> maximum. Let the slope of this line be S, at a potential of $\phi_{LOG}$.

3. Compute electron temperature $T_e$ from Eq. (8).

4. Compute

$$\phi_o = \frac{\phi_{LIN} + \phi_{LOG}}{2} = -\phi_s \tag{12}$$

5. Interpolate to find:

   measured current $I_o$, at $\phi_p = \phi_o$

   measured current $I_R$, at $\phi_p = R$

13

6. Compute electron density $N_e$ from

$$N_e = \frac{2 I_O \sqrt{\pi} \times 10^6}{A e \alpha a} \quad cm^{-3} \tag{13}$$

($T_e$ obtained from step 3 is used to compute a.)   Numerically,

$$N_e = -6.896 \times 10^9 \ I_O \ S \ cm^{-3} \tag{14}$$

Thus we now have $N_e(t_O)$, $T_e(t_O)$ and $\phi_s(t_O)$ at a time $t_O$ which can be equated to the midpoint of the sweep

$$t_O = \frac{t_s + t_e}{2} \ , \tag{15}$$

where $t_s$ and $t_e$ are times of start and end of sweep, respectively.

7. Calculate the electron density during Mode 1 operation using Eq. (11).

The density is calculated during the following 118 sec of Mode 1 (M1EL) operation by assuming that the temperature $T_e$ and vehicle potential $\phi_s$ are constant between sweeps (Mode 2).

## 3. THE ION SENSOR

The ion sensor is a planar aperture, planar collector sensor, a cross section of which is shown in Figure 7. It is mounted on the 2.5-ft rigid boom shown in Figure 5 and located so that it faces into the spacecraft velocity vector at all times. The 1.00 in. diam aperture is covered by a double grid of gold plated tungsten wire. The double grid is used to minimize electric field leakage that would disturb the trajectories of incoming positive ions. Like the electron sensor, the ion sensor has two modes of operation which alternate automatically (see Figure 3 and Table 1). In Mode 1, the retarding (swept) grids in Figure 7 are electrically connected to the spacecraft frame and all ions passing through the aperture are collected. The ion sensor Mode 1 is used to measure instantaneous ion densities. The retarding grids are swept once every 128 sec from -5 V to +12 V (Mode 2) to obtain ion temperature. This swept grid is also a double grid to improve the uniformity and accuracy of the applied potential across its surface. Between the retarding grids and the collector, a third grid is maintained negative with respect to the collector at all times. This acts as a suppressor to the photoelectrons and secondary electrons generated at the collector by solar UV and energetic particles, respectively.

14
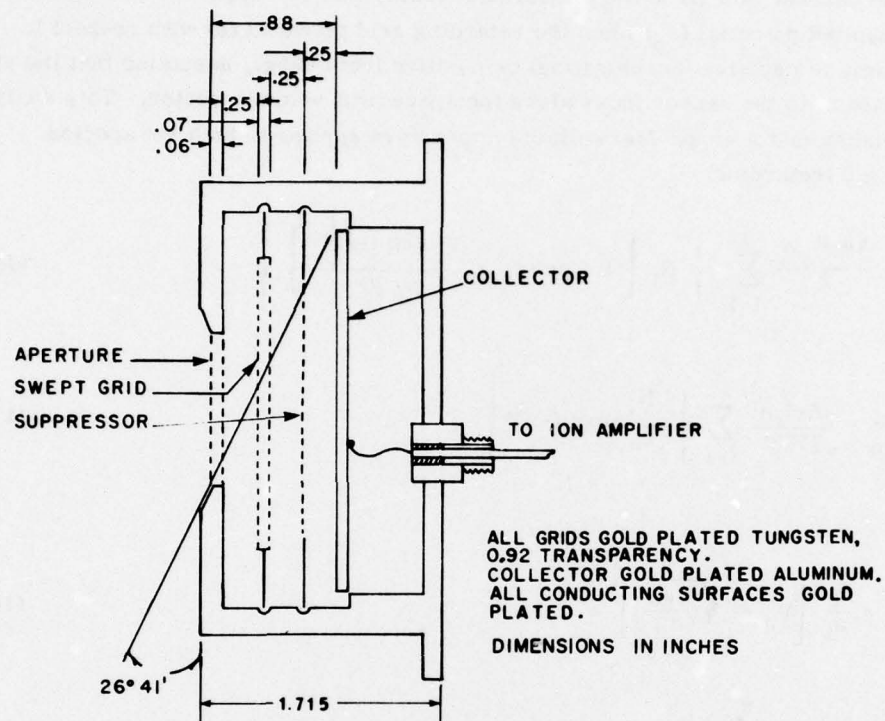
Figure 7. Cross Section of SSIE Ion Sensor

These would otherwise appear as unwanted positive currents in the amplifying system. As shown in Figure 3, the voltages between the different components of the ion sensor are maintained constant at all times, including the sweep periods, in order to avoid variations in the collected current due to variations within the sensor. All conducting components of the sensor are gold plated to minimize contact potential effects.

The analysis of the fixed voltage (Mode 1) data is given in Eqs. (19) and (38) for the two ion species and single ion species cases, respectively. The theory of the analysis of the swept voltage (Mode 2) data is given in Section 3.1 and the theory for the scale height determination, in Section 3.3.

### 3.1 Sweep Mode Analysis (Mode 2)

The current flow (I) to the (planar) ion sensor can be expressed as a function of the applied potential $(\phi_p)$ when the retarding grid potential $(\phi)$ with respect to the plasma is negative (accelerating) or positive (retarding), assuming that the outward normal to the sensor looks along the spacecraft velocity vector. This analysis assumes that a single Maxwellian temperature applies to both ion species. For $e\phi \geq 0$ (retarding)

$$I = \frac{Ae\,V_s\,\alpha}{2} \sum_{i=1}^{j} \left\{ N_i \left[ 1 + \text{erf}(x_i) + \frac{a_i \exp(-x_i^2)}{V_s\sqrt{\pi}} \right] \right\} \tag{16}$$

$$\frac{\partial I}{\partial \phi_p} = \frac{Ae^2\,\alpha}{\sqrt{2\pi kT}} \sum_{i=1}^{j} \left\{ \frac{N_i}{\sqrt{m_i}} \exp(-x_i^2) \right\} \tag{17}$$

where

$$x_i = \frac{1}{a_i} \left[ V_s - \sqrt{\frac{2e\phi}{m_i}} \right] \tag{18}$$

$$\text{erf}(x) = \frac{2}{\sqrt{\pi}} \int_0^x \text{erp}(-z^2)\,dz \quad \text{(definition)}$$

$\phi$ = potential of sensor with respect to plasma = $\phi_s + \phi_p$ (volts)

$\phi_s$ = potential of vehicle with respect to plasma (volts)

$\phi_p$ = sensor potential with respect to vehicle (volts)

A = sensor aperture area ($m^2$) = $\pi r^2$, where r is aperture radius = 0.0127 m

e = electronic charge = $1.602 \times 10^{-19}$ coulomb

$\alpha$ = sensor transparency = 0.590

$N_i$ = ambient ion density of $i^{\text{th}}$ constituent ($m^{-3}$)

$m_i$ = mass of $i^{\text{th}}$ constituent (kg)

$a_i$ = $(2kT/m_i)^{1/2}$ = most probable speed of $i^{\text{th}}$ constituent (m sec$^{-1}$)

T = average ion temperature of all constituents ($^{\circ}$K)

k = Boltzmann constant = $1.38054 \times 10^{-23}$ joule/$^{\circ}$K

16

$j$ = number of ion constituents

$V_s$ = vehicles speed (m sec$^{-1}$) = 7437 m sec$^{-1}$

For $e\phi < 0$ (accelerating) on the retarding grid, the current collected is only a function of the flux of ions through the aperture. Put $\phi = 0$ in retarding Eq. (16) and $x_i = V_s/a_i$ in Eq. (18). Then I is constant (not a function of $\phi_p$) and so

$$\frac{\partial I}{\partial \phi_p} = 0 \quad .$$

### 3.1.1 TWO SPECIES CASE

To handle this complicated expression, it will be assumed that for the DMSP satellite altitude (circular orbit) of 835 km we have, at <u>most</u>, two ion species, namely, $H^+$ and $0^+$. Of course, we must allow for either, or both to be present: thus for $j = 2$, $m_1 = 1.66035 \times 10^{-27}$ kg, $m_2 = (16) \times (1.66035 \times 10^{-27}$ kg) and for $j = 1$, either $m_1 = (1) m_p$ or $m_1 = (16) m_p$, where $m_p = 1.66035 \times 10^{-27}$ kg.

To gain an understanding of the behavior of the current flow as a function of the applied voltage on the retarding grid, let us for the moment consider what the response would be if $V_s \gg a$ (very low ion temperature T), and we have two components present, where $m_2 > m_1$.

For $0 < \phi < m_1 V_s^2/2$ e , $x_1$ and $x_2 \gg 1$, erf $(x_1)$ = erf $(x_2)$ = 1, exp $(-x_1^2)$ = exp $(-x_2^2)$ = 0, we find that

$$I = Ae \, V_s \, \alpha \, (N_1 + N_2) \tag{19}$$

For $m_1 V_s^2/2$ e $< \phi < m_2 V_s^2/2$ e, $x_1 \ll -1$, $x_2 \gg 1$, erf $(x_1)$ = -1, erf $(x_2)$ = 1, exp $(-x_1^2)$ = exp $(-x_2^2)$ = 0 we find that

$$I = Ae \, V_s \, \alpha N_2 \tag{20}$$

For $\phi > m_2 V_s^2/2$ e, $x_1$ and $x_2 \ll -1$, erf $(x_1)$ = erf $(x_2)$ = -1, exp $(-x_1^2)$ = exp $(-x_2^2)$ = 0, we find that

$$I = 0$$

These three operating regimes are shown graphically in Figure 8.

$Ae V_s \propto (N_1 + N_2)$

$Ae V_s \propto N_2$

$\phi_1 = \dfrac{m_1 V_s^2}{2e}$

$\phi_2 = \dfrac{m_2 V_s^2}{2e}$
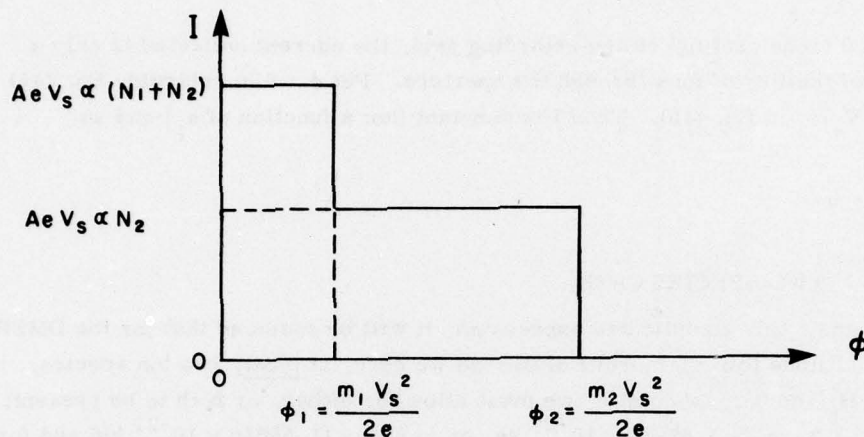
Figure 8. Ion Sensor Current vs Applied Voltage for Two Species

Since the orbit is circular, $V_s$ is constant = 7.437 km sec$^{-1}$ ($\tau$, orbital period = 101 min 28 sec), and we can calculate from Eq. (18)

$$\phi_1 = \frac{(1.660 \times 10^{-27})(7.437 \times 10^3)^2}{2x\,(1.602 \times 10^{-19})} = 0.287 \text{ V} \tag{21}$$

and

$$\phi_2 = (16)\,\phi_1 = 4.586 \text{ V} \quad . \tag{22}$$

These are the two points that give $x_1 = 0$ and $x_2 = 0$, respectively. It can easily be seen from Eq. (18) that, because $1/a_i$ occurs as a multiplier on $[V_s - \sqrt{2}\,e\phi/m_i]$, $\phi_1$ and $\phi_2$ give zero for $x_1$ and $x_2$, respectively, for all $a_i$ (all T). Examining the second derivative of I (for one species), we note

$$\frac{\partial^2 I}{\partial \phi_p^2} = \frac{-Ae^2\,\alpha N}{kT} \quad \frac{2\,e}{\pi m \phi} \times e^{-x^2} \quad ; \tag{23}$$

it is obvious that $\partial^2 I / \partial \phi_p^2 = 0$ when $x = 0$; hence the first derivative reaches a <u>minimum</u> value at $x = 0$.

18

Thus as the temperature is increased from the previously assumed small value, the slopes at $\phi_1$ and $\phi_2$ increase from $-\infty$, but the slope always reaches its maximum negative value at $\phi_1$ and $\phi_2$ and can be directly related to the density and mass of each species and their temperatures. For illustrative purposes, Figure 9 shows a plot of I, $\partial I/\partial \phi_p$ and $\partial^2 I/\partial \phi_p^2$, assuming equal densities of $10^3$ cm$^{-3}$ for each species with a temperature of 3000°K and vehicle potential of -2 V (the curves were computed with $V_s = 7.22$ km sec$^{-1}$ as opposed to correct value of 7.437 km sec$^{-1}$, but this merely shifts $\phi_1$ and $\phi_2$ a slight amount and does not change the character of the curves).[*] It can be seen from Figure 9 that I is determined solely by species $(0^+)$ when $\phi_p > 4.5$ V. Because of the behavior of erf (x) and exp $(-x^2)$, the slope $\partial I/\partial \phi_p$ is determined solely by one species or the other in the vicinity of $\phi_1$ or $\phi_2$; (that is, by $H^+$ when $\phi_p < 4$ V and by $0^+$ when $\phi_p > 4.5$ V). The relative contributions of the two species can be clearly separated.

Figure 10 illustrates Log I vs applied voltage for the same data. For comparison, the electron sensor response of Log (I) as a function of $\phi_p$ is also shown in Figure 10. It is clear that no useful data can be extracted for the ion Log I curve (as opposed to the case for electrons where the slope is inversely proportional to $T_e$).

Writing out the separate contributions of the two species at $x_1 = 0$ and $x_2 = 0$, respectively, we have:

at $x_1 = 0$, $\phi = \phi_1 + \phi_s$

$$I_1 = \frac{Ae\,V_s\,\alpha N_1}{2}\left[1 + \frac{a_1}{V_s\sqrt{\pi}}\right] \tag{24}$$

$$\frac{\partial I_1}{\partial \phi_p} = \frac{-Ae^2\,\alpha N_1}{2}\sqrt{\frac{2}{\pi kT\,m_p}} = S_1 \tag{25}$$

$$V_s - \sqrt{\frac{2\,e\,(\phi_1 + \phi_s)}{m_p}} = 0 \tag{26}$$

$$a_1 = \sqrt{\frac{2kT}{m_p}} \tag{27}$$

---

[*]Curves for the single species case are denoted by (a).

19
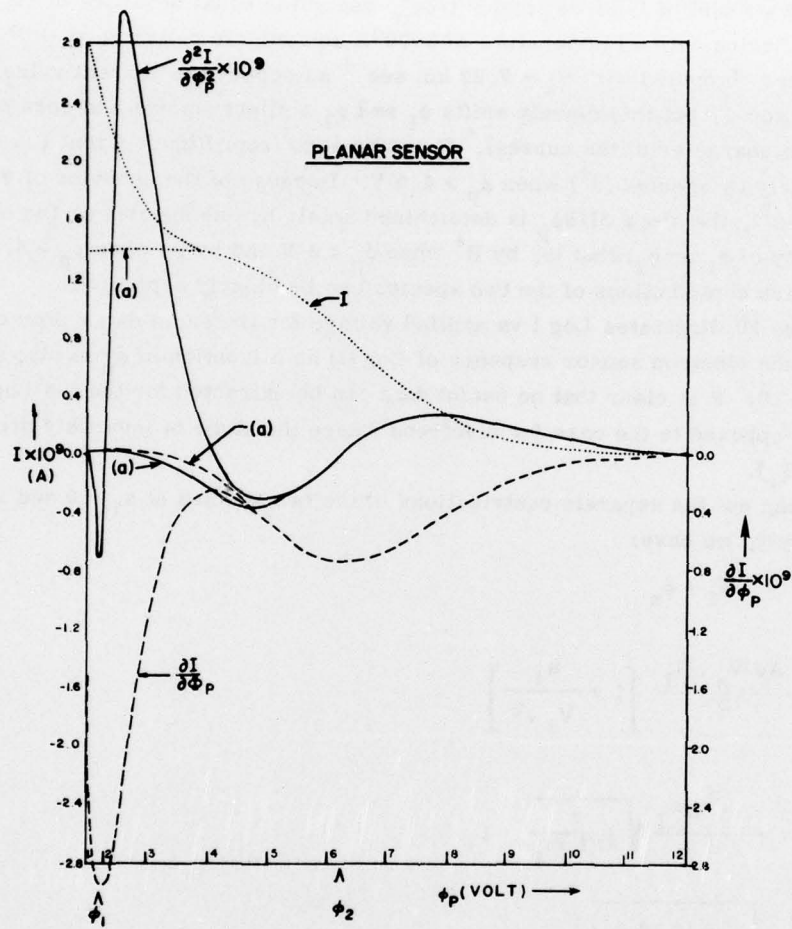
Figure 9. Ion Sensor Theory: $I_+$ vs $\phi_p$ and Derivatives
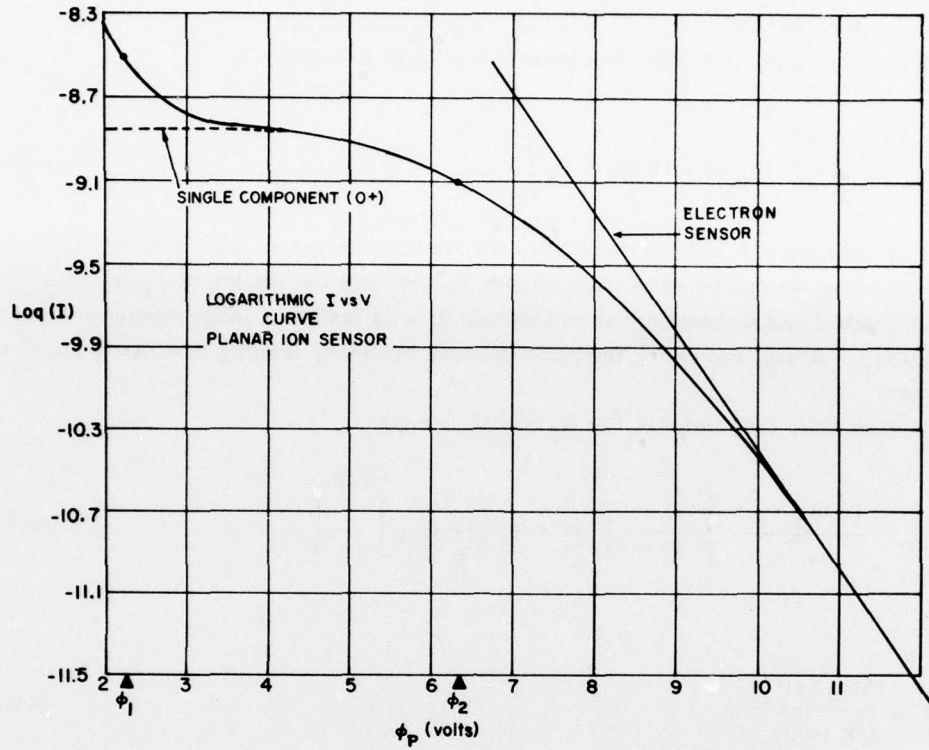
Figure 10. Ion Sensor Theory: $Log_{10} (I_+)$ vs $\phi_p$

and at $x_2 = 0$, $\phi = \phi_2 + \phi_s$

$$I_2 = \frac{Ae\ V_s\ \alpha N_2}{2} \left[1 + \frac{a_2}{V_s\ \sqrt{\pi}}\right] \tag{28}$$

$$\frac{\partial I_2}{\partial \phi_p} = \frac{-Ae^2\ \alpha N_2}{2} \sqrt{\frac{2}{\pi kT\ 16\ m_p}} = S_2 \tag{29}$$

$$V_s - \sqrt{\frac{2\ e\ (\phi_2 + \phi_s)}{16\ m_p}} = 0 \tag{30}$$

$$a_2 = \sqrt{\frac{2kT}{16\ m_p}} \tag{31}$$

21

Thus, identifying the values of $\phi_p$, $I$ and $\partial I / \partial \phi_p$ at which the slope S is a maximum negative value, we obtain $\phi_1$, $I_1$, $\partial I_1 / \partial \phi_p$, $\phi_2$, $I_2$ and $\partial I_2 / \partial \phi_p$.

From Eqs. (26) and (30), we obtain the vehicle potential

$$V_s = \frac{1}{2} \left[ \frac{V_s^2}{2e} m_p (1 + 16)(\phi_1 + \phi_2) \right] \tag{32}$$

To get temperature T and the densities, we shall make use of Eqs. (28) and (29) only, because, as can be seen from Figure 9, the first derivative at $\phi_1$ is quite sharply peaked and a small error in location $\phi_1$ will lead to a large error in deducing $\partial I_1 / \partial \phi_p$. At $\phi_2$, however, the peak is much broader, leading to a much greater accuracy.

Solving Eqs. (28) and (29) for $N_2$ and T, we get

$$N_2 = \frac{16 \, m_p \, S_2 \, \pi}{Ae^2 \, \alpha} \left\{ \frac{-V_s}{2} + \left[ \frac{V_s^2}{4} + \frac{2 \, I_2 \, e}{16 \, m_p \, S_2 \, \pi} \right]^{1/2} \right\} \tag{33}$$

and

$$T = \frac{(Ae \, \alpha N_2)^2 \, e^2}{2 \pi k \, 16 \, m_p \, S_2^2} \tag{34}$$

For $N_1$ we could use Eq. (24), since T is now known, hence $a_1$ is known, but again, since the slope at $\phi_1$ is so steep, the value of $I_1$ will be susceptable to error. A more accurate value of $N_1$ will be obtained by reading off the current $I_o$ at $\phi_p = -\phi_s$ (we now know the value of $\phi_s$), that is, the current at $\phi = 0$ given by

$$I_o = \frac{Ae \, V_s \, \alpha}{2} \left\{ N_1 \left[ \cdot 1 + \text{erf} \, (V_s/a_1) + \frac{a_1 \, \exp \, (-V_s^2/a_1^2)}{V_s \, \sqrt{\pi}} \right] \right.$$

$$\left. + N_2 \left[ 1 + \text{erf} \, (V_s/a_2) + \frac{a_2 \, \exp \, (-V_s^2/a_2^2)}{V_s \, \sqrt{\pi}} \right] \right\} \tag{35}$$

where $a_1$ and $a_2$ are defined in Eqs. (27) and (31).

22

Thus

$$N_1 = \frac{\dfrac{2\,I_o}{Ae\,V_s\,\alpha} - N_2 \left[ 1 + \mathrm{erf}\,(V_s/a_2) + \dfrac{a_2\,\exp\,(-V_s^2/a_2^2)}{V_s\,\sqrt{\pi}} \right]}{1 + \mathrm{erf}\,(V_s/a_1) + \dfrac{a_1\,\exp\,(-V_s^2/a_1^2)}{V_s\,\sqrt{\pi}}} \qquad (36)$$

We can simplify this expression slightly by noting that $(V_s/a_2)$ has the smallest value for largest T. If we take $T = 10^4\,^\circ$K which is an extremely high value, then $a_2 = 3224$ m sec$^{-1}$, $(V_s/a_2) = 2.307$, $\mathrm{erf}\,(V_s/a_2) = 0.999$, and $\exp\,(-V_2^2/a_2^2) = 4.884 \times 10^{-3}$ giving

$$1 + \mathrm{erf}\,(V_s/a_2) + \frac{a_2\,\exp\,(-V_s^2/a_2^2)}{V_s\,\sqrt{\pi}} = 2.000094 \approx \underline{2} \quad .$$

For a lower temperature, $(V_s/a_2)$ becomes larger, giving a value even closer to 2. Because $(V_s/a_1) = 0.577$ and $\mathrm{erf}\,(V_s/a_1) \approx 0.585$, we cannot reduce Eq. (36) any further, and thus

$$N_1 = \left[ \frac{2\,I_o}{Ae\,V_s\,\alpha} - 2\,N_2 \right] \Bigg/ \left[ 1 + \mathrm{erf}\,(V_s/a_1) + \frac{a_1\,\exp\,(-V_s^2/a_1^2)}{V_s\,\sqrt{\pi}} \right] \qquad (37)$$

### 3.1.2 SINGLE SPECIES CASE

The case where just one ion species is present cannot be handled by the previous analysis because that depends on locating two maximum negative slope points where the first point at $\phi_1$ can be identified as associated with H$^+$, and the second point $\phi_2$ with $0^+$. If, however, only a single minimum slope point is identified, it is not known a priori whether this point is $\phi_1$ or $\phi_2$. To illustrate, in Figure 10, is we identify a maximum negative slope only at $\phi_p = 6.321$ volts, we do not know whether the species is $0^+$, giving a vehicle potential $\phi_s = -2$ volts or H$^+$, giving a vehicle potential of -5.052 volts. The corresponding temperatures work out to be $3000^\circ$K and $1330^\circ$K, respectively. Essentially, we have to choose a single set of equations, (24), (25), (26) or (28), (29), (30), depending upon whether the mass is $m_p$ or 16 $m_p$ (H$^+$ or $0^+$). The clue to choosing the correct set is to make use of the fact that when $\phi < 0$, the current is constant:

23

$$I_o = \frac{Ae\ V_s\ \alpha}{2}\ N_1 \left[ 1 + \text{erf}\ (V_s/a_1) + \frac{a_1\ \exp\ (-V_s^2/a_1^2)}{V_s\ \sqrt{\pi}} \right] \quad . \tag{38}$$

Here $N_1$ and $a_1$ refer to the now single species. This equation, together with equations at $\phi_p = \phi$, (maximum negative slope) $= \phi_{min}$

$$I_1 = \frac{Ae\ V_s\ \alpha N_1}{2} \left[ 1 + \frac{a_1}{V_s\ \sqrt{\pi}} \right] \tag{39}$$

$$\frac{\partial I_\sigma}{\partial \phi_p} = S_1 = \frac{-Ae^2\ \alpha N_1}{2} \sqrt{\frac{2}{\pi kT\ m_1}} \tag{40}$$

$$V_s - \sqrt{2\ e\ \frac{(\phi_{min} + \phi_s)}{m_1}} = 0 \tag{41}$$

are solvable <u>numerically</u> for the four unknowns $N_1$, $T$, $m_1$, and $\phi_s$, but certainly not algebraically because the equation in $I_o$ is nonlinear.

There are two ways around this difficulty and both ways will be used in the data reduction scheme:

1. Make use of $N_e$ derived from the preceding electron sweep, and set $N_1 = N_e$ in Eq. (38).

2. Assume that the ion temperature $T$ is going to be less than $3000^o$K. Then the maximum value of $a_1$ will be given by

$$a_1 = \sqrt{\frac{2\ k\ (3000)}{m_p}} = 7.063 \times 10^3 \quad ,$$

giving

$$\left[ 1 + \text{erf}\ (V_s/a_1) + \frac{a_1\ \exp\ (-V_s^2/a_1^2)}{V_s\ \sqrt{\pi}} \right] = 2.0404 \approx 2 \quad .$$

This is a worst-case and value gets closer to 2 for $T < 3000^o$K and is very close for $0^+$ ($m_1 = 16\ m_p$).

24

With this approximation, Eq. (38) becomes

$$I_o = Ae\ V_s\ \alpha N_1$$

and is independent of mass giving directly

$$N_1 = I_o/Ae\ V_s\ \alpha$$

Either case (1) or (2) yields the value of N, which is then used in Eqs. (39) and (40) to give

$$m_1 = \frac{(Ae\ \alpha N_1)^2\ e}{2S_1\ \pi\ \left[I_1 - \dfrac{Ae\ V_s\ \alpha N_1}{2}\right]}\ kg \tag{42}$$

or, in atomic mass units

$$M_1 = \frac{(Ae\ \alpha N_1)^2\ e}{2\ S_1\ \pi\ \left[I_1 - \dfrac{Ae\ V_s\ \alpha N_1}{2}\right]\ m_p}\ AMU \tag{43}$$

This value is then used to calculate

$$T = \frac{(Ae\ \alpha N_1)^2\ e^2}{2\pi k\ M_1\ m_p\ S_1^2} \tag{44}$$

and

$$\phi_s = \left[\frac{V_s^2}{2e}\ M_1\ m_p - \phi_1\right] \tag{45}$$

### 3.2 Ion Data Reduction Procedure

The foregoing analysis then leads to the following data reduction procedure:

1. Take the measured current I as a function of $\phi_p$. Working from the start of the sweep in time ($\phi_p = -5$ V) and disregarding current readings when the telemetry scale is saturated, one should fit a straight line to 3 data points to determine the slope and then move the fitting process through the entire sweep, one point at a time.

Find the center point at which the slope reaches its first maximum negative value ($\phi_1$) and its second maximum negative value ($\phi_2$), and let the slopes be $S_1$ and $S_2$, respectively. Take also the currents $I_1$ and $I_2$ at $\phi_1$ and $\phi_2$. If only one maximum negative slope can be located, proceed to step 4; otherwise go to step 2.

2. Compute vehicle potential $\phi_s$ given by Eq. (32)

$$\phi_s = \frac{1}{2} \left[ \frac{17 \, V_s^2 \, m_p}{2 \, e} - (\phi_1 + \phi_2) \right]$$

and read off (interpolate) measured current ($I_o$) at $\phi_p = -\phi_s$.

3. Compute $N_2$, $N_1$, T given by Eqs. (33), (37), (34)

$$N_2 = \frac{16 \, m_p \, S_2 \, \pi}{e^2 A \, \alpha} \left\{ - \frac{V_s}{2} + \left[ \frac{V_s^2}{4} + \frac{2 \, I_2 \, e}{16 \, m_p \, S_2 \, \pi} \right]^{1/2} \right\}$$

$$N_1 = \left[ \frac{2 \, I_o}{Ae \, V_s \, \alpha} - 2 \, N_2 \right] \Bigg/ \left[ 1 + \text{erf} \, (V_s/a_1) + \frac{a_1 \, \exp \, (-V_s^2/a_1^2)}{V_s \, \sqrt{\pi}} \right]$$

$$T = \frac{(Ae \, \alpha N_2)^2 \, e^2}{2 \, \pi \, k \, 16 \, m_p \, S_2^2}$$

and from $N_1$ and $N_2$ we obtain the average ion mass

$$M_{ave} = \frac{(N_1 + 16 \, N_2)}{N_1 + N_2} \, \text{AMU} \tag{46}$$

Go to step 6.

4. Read off the current ($I_o$) at $\phi_p = 0$ volts and compute $N_1 = I_o/Ae \, V_s$.

5. Compute $M_1$, T and $\phi_s$ given by Eqs. (43), (44), and (45),

$$M_1 = \frac{(Ae \, \alpha N_1)^2 \, e}{2 \, S_1 \, \pi \left[ I_1 - \dfrac{Ae \, V_s \, \alpha N_1}{2} \right] m_p} \, \text{AMU}$$

26

$$T = \frac{2(Ae\ \alpha N_1)^2\ e^2}{2\pi k M_1 m_p S_1^2}\ {}^{\circ}K$$

$$\phi_s = \left[ \frac{V_s^2 M_1 m_p}{2\ e} - \phi_1 \right]\ volts$$

Repeat step 5 with $N_1 = N_e$ (value from previous electron sweep M2EL) generating a second set of values $M_1^e$, $T^e$, $\phi_s^e$. The two sets of values for the single species ion mass, temperature, and vehicle potential can be compared. Ideally, the two sets will be identical but, in fact, they occasionally differ and both sets of values are made available for a later decision as to the best values.

6. We now have a set of ion parameters. Since the center of the ion Mode 2 sweep occurs 17 sec after the electron Mode 2 sweep, these ion parameters are assumed to be valid at time $= t_o + 17$ sec. Thus,

$$N_i(t_o + 17\ sec) = N_1 + N_2\ or\ N_1\ or\ N_e$$

$$M_i(t_o + 17\ sec) = M_{ave}\ or\ M_1\ or\ M_1^e$$

$$T_i(t_o + 17\ sec) = T\ or\ T^e$$

$$\phi_s(t_o + 17\ sec) = \phi_s\ or\ \phi_s^e$$

where $t_o$ is the time of the center of the previous electron sweep. During the ion Mode 1 period, the instantaneous total ion density is obtained from Eq. (19) as

$$N(t) = N_1(t) + N_2(t) = I(t)/Ae\ V_s\ \alpha \tag{47}$$

### 3.3 Electrostatic Field Penetration

It has been shown[1,2] that the electrostatic potential in the spacings of a planar sensor's grids is a function both of the electrostatic potential applied to the grid wires and of the electrostatic potential of adjacent grids. The potential in the spacing

1. Hanson, W. B., Frame, D. R., and Midgley, J. E. (1972) Errors in retarding potential analyzers caused by nonuniformity of the grid-plane potential, J. Geophys. Res. 77(No. 10):1914-1922.

2. Goldan, P. D., Yadlowsky, E. J., and Whipple, E. C., Jr. (1973) Errors in ion and electron temperature measurements due to grid plane potential nonuniformities in retarding potential analyzers, J. Geophys. Res. 78(No. 16): 2907-2916.

27

is the effective potential ($\phi_{eff}$) of the grid; it should be used in the above data analysis equations. The effective potential on a grid "i" is approximately given by

$$\phi_{eff_i} = V_i + \varepsilon (V_{i-1} - 2 V_i + V_{i+1}) \tag{48}$$

where

$V_i$ = the applied potential to grid i

$V_{i-1}$ = the applied potential to the grid in front of grid i

$V_{i+1}$ = the applied potential to the grid behind grid i

$\varepsilon$ = field penetration factor

In theory, $\varepsilon$ can be calculated from the spacing of the grids and the dimensions of the grid wires. In practice, $\varepsilon$ must be adjusted to fit the characteristics of the instrument. For this instrument with its double grids, theory gives $\varepsilon \lesssim 0.06$, but in practice $\varepsilon$ may be as great as 0.12.

For the DMSP sensor, let us assume that the thickness of the sheath outside the aperture is approximately equal to the grid spacing. Thus the applied voltages of interest are

| | |
|---|---|
| i = 0 is the plasma | $V_o = 0$ |
| i = 1 is the aperture grid | $V_1 = \phi_s$ |
| i = 2 is the retarding grid | $V_2 = V + \phi_s$ |
| i = 3 is the suppressor grid | $V_3 = V + \phi_s - 30$ |

where V is sweep voltage applied to retarding grid.

From Eq. (48), the effective potential on the aperture grid is

$$\phi_A = \phi_s (1 - \varepsilon) + \varepsilon V \tag{49}$$

and the effective potential on the retarding grid is

$$\phi_R = \phi_s + V (1 - \varepsilon) - 30 \varepsilon \tag{50}$$

The flow of ions to the collector plate is regulated by the grid with the most positive electrostatic potential. Table 2 shows the effective potentials as a function of the applied retarding potential for $\phi_s = -2$ V and $\varepsilon = 0.06$ and $\varepsilon = 0.12$. When $\phi_A \geq \phi_R$, the effective potential on the aperture controls the current, and when $\phi_A \leq \phi_R$, the effective potential on the retarding grid controls the current. In the data analysis, the effective potential controlling the ion current should be used

28

Table 2. Effective Electrostatic Potential for Planar Sensor

| Applied Voltage | Effective Potential | | | |
| | $\epsilon = 0.06$ | | $\epsilon = 0.12$ | |
| (V) | $\phi_A$ (V) | $\phi_R$ (V) | $\phi_A$ (V) | $\phi_R$ (V) |
|---|---|---|---|---|
| -5 | -2.180 | -8.500 | -2.360 | -10.000 |
| -4 | -2.120 | -7.560 | -2.240 | -9.120 |
| -3 | -2.060 | -6.620 | -2.120 | -8.240 |
| -2 | -2.000 | -5.680 | -2.000 | -7.360 |
| -1 | -1.940 | -4.740 | -1.880 | -6.480 |
| 0 | -1.880 | -3.800 | -1.760 | -5.600 |
| 1 | -1.820 | -2.860 | -1.640 | -4.720 |
| 2 | -1.760 | -1.920 | -1.520 | -3.840 |
| 2.182 | -1.749 | -1.749 | -- | -- |
| 3 | -1.700 | -0.980 | -1.400 | -2.960 |
| 4 | -1.640 | -0.040 | -1.280 | -2.080 |
| 5 | -1.580 | 0.900 | -1.160 | -1.200 |
| 5.053 | ... | ... | -1.154 | -1.154 |
| 6 | -1.520 | 1.840 | -1.040 | -0.320 |
| 7 | -1.460 | 2.780 | -0.920 | 0.560 |
| 8 | -1.400 | 3.720 | -0.800 | 1.440 |
| 9 | -1.340 | 4.660 | -0.680 | 2.320 |
| 10 | -1.280 | 5.600 | -0.560 | 3.200 |
| 11 | -1.220 | 6.540 | -0.440 | 4.080 |
| 12 | -1.160 | 7.480 | -0.320 | 4.960 |
| 13 | -1.100 | 8.420 | -0.200 | 5.840 |
| 14 | -1.040 | 9.360 | -0.080 | 6.720 |

instead of the applied voltage on the retarding grid. Use of the uncorrected retarding grid voltage yields ion temperatures that are too high by 10 to 40 percent.

## 4. PLASMA SCALE HEIGHT DETERMINATION

There is sufficient information from the analysis of the electron Mode 2 and ion Mode 2 data to compute[3] the plasma scale height $H_p$ at a time centered on the two swept voltage modes which occur 17 sec apart; that is, $H_p$ is determined at $(t_o + 8.5)$, where $t_o$ is center of an electron sweep, to be

$$H_p(t_o + 8.5) = k(T_e + T)/M_i \, m_p \, g \quad km \tag{51}$$

where $g$ = acceleration due to gravity at 835 km altitude $(km/sec^2)$;
$$g = 7.675 \, 10^{-3} \, km/sec^2$$
Substitute in constants

$$H_p(t_o + 8.5) = 1.083 \left(\frac{T_e + T}{M_i}\right) \quad km \quad . \tag{52}$$

## 5. TELEMETRY ALLOCATIONS AND ELECTRONICS

With the exception of two housekeeping data words, all the data from the SSIE experiment is transmitted via the spacecraft digital data systems (OLS) using a single NRZ (nonreturn to zero) data signal. This signal is transferred once per second in phase with the OLS supplied bit clock in bursts of 180 contiguous bits at a rate of 1000 ± 1 bps as shown in Figure 11. Upon receipt of a read pulse (SSIERED) from the OLS, the SSIE experiment provides 180 data bits with the least significant bit occurring first in the first word. These 180 data bits form twenty 9-bit data words.

The outputs from the three experiments are equally spaced throughout the 1-sec interval and arranged in the twenty data words as follows:

| Type | No. Samples | Words |
|------|-------------|-------|
| Electron sensor data | 7 | 1, 4, 7, 10, 13, 16, 19 |
| Ion sensor data | 7 | 2, 5, 8, 11, 14, 17, 20 |
| Event monitor | 6 | 3, 6, 9, 12, 15, 18 |

---

3. Rishbeth, H., and Garriott, O.K. (1969) Introduction to Ionospheric Physics, Academic Press, New York, p. 143.
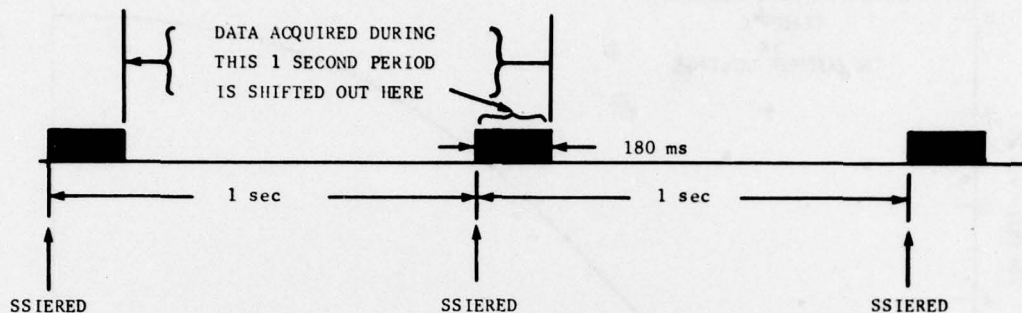
30

Figure 11.   SSIE Telemetry Word Transfer

The electron and ion sensor data words are converted from a telemetry output voltage to an amplifier current using preflight and in-flight calibrations.   This procedure is described in Section 5.2.

The event monitor is an analog indicator of the voltage applied to both the electron and ion sensors during their respective sweep periods.   The actual voltage to the sensor components is derived by fitting a straight line to the event monitor analog voltage and then comparing it with a preflight calibration of applied volts vs analog volts.

The event monitor also indicates calibration sequences and "flags" the sweep periods 2 sec prior to the sweep, as an aid to data processing.   It should be noted that all events, such as calibrates, sweeps and flag voltages first appear at word 18 of the 20-word, 180-bit burst of data.   Therefore the first words of data from a sweep or calibrate are words 19 and 20 for the electron and ion sensors, respectively.

The two housekeeping quantities which are transmitted using the spacecraft analog system are:

Word 48 - Output voltage of thermistor in main electronics package.
          Calibration given in Figure 12.

Word 49 - Monitor of bias voltage applied to grid of electron sensor.
          Values given in Table 1.

### 5.1  Time Sequence of Events

Figure 13 shows the sequence of all functions of the Event Monitor, Electron Sensor and Ion Sensor.   At all other times, the sensors themselves are operating and recording data in the fixed voltage mode.   Additional information is listed in Table 1, including in-flight calibrate details and the designation of the telemetry output for the electron grid resting bias voltage.

31

BLOCK 5D, F2 SPACECRAFT
TEMP-°C
vs.
TM OUTPUT VOLTAGE

Figure 12.   Thermistor Calibration



NOTES:

1. ELEC. SENSOR, DURING BIAS MODE I, +1.5 V APPLIED TO OUTER GRID. DURING BIAS MODE 2, 0V APPLIED TO OUTER GRID.

2. ELEC. SENSOR COLLECTOR IS BIASED AT + 20 V W.R.T. OUTER GRID AT ALL TIMES INCLUDING SWEEP PERIODS.

3. ION SENSOR SUPPRESSOR GRID AND COLLECTOR ARE BIASED AT - 30 V AND - 20 V RESPECTIVELY W.R.T. SWEPT GRID AT ALL TIMES INCLUDING SWEEP PERIODS.
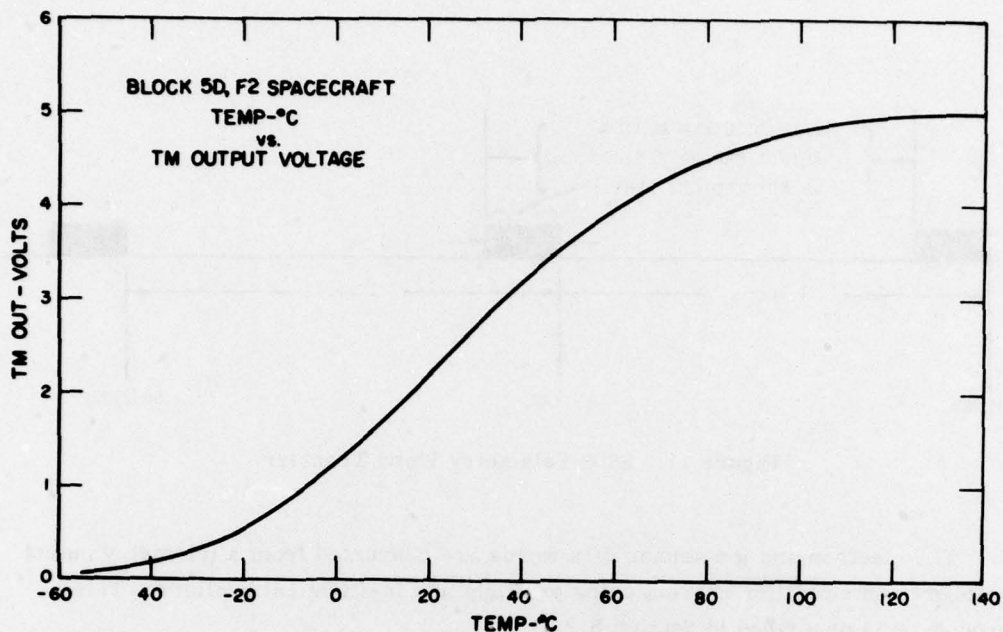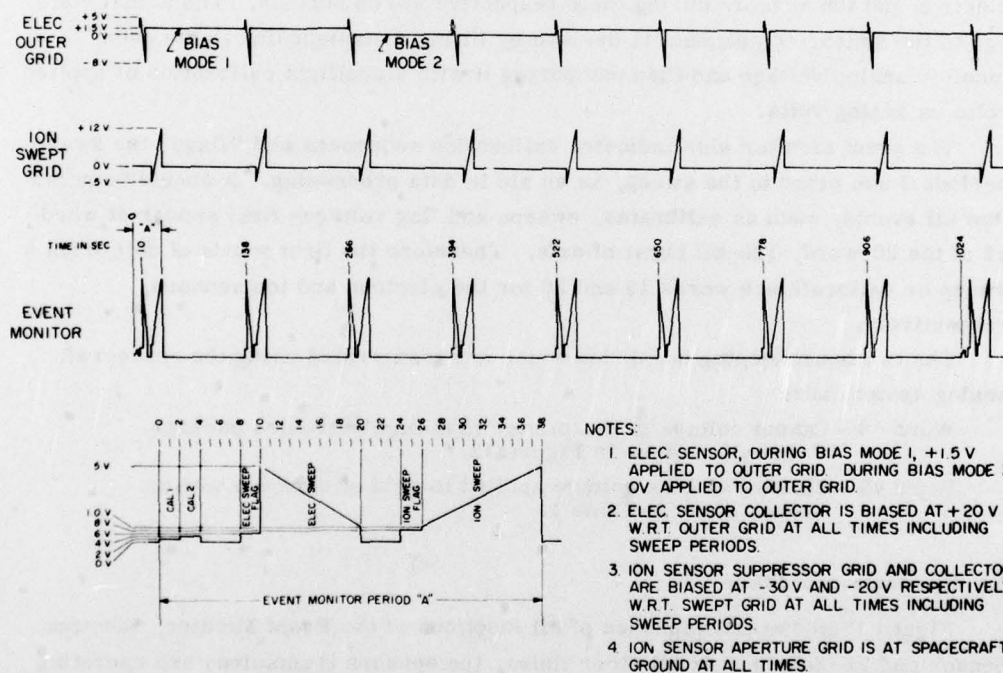
4. ION SENSOR APERTURE GRID IS AT SPACECRAFT GROUND AT ALL TIMES.

SSI/E TIMING SCHEME
DMSP BLOCK 5D F2 SPACECRAFT ONLY

Figure 13.   SSIE Time Sequence of Events

32

### 5.2 Preflight Calibration and In-flight Update

Before integration with the spacecraft, the amplifiers were accurately calibrated for response to known input currents over a wide range of temperatures. The preflight calibrations are shown in Figures 14 and 15 and in Tables 3 and 4, for a temperature of $+20^{\circ}C$. Both amplifiers have a logarithmic response with outputs 0 to 5 V for ranges $10^{-10}$-$10^{-5}$ A in the electron (negative current) amplifier case, and $5 \times 10^{-12}$-$5 \times 10^{-7}$ A in the case of the ion (positive current) amplifier.

These amplifier responses may be expressed as

$$Log(I) = A + BV \tag{53}$$

where $Log(I)$ is $Log_{10}$ of the input current; V is output voltage of amplifier to telemetry; and A and B are constants.

Using e and i as subscripts to denote the electron and ion current amplifiers, from the preflight calibrations, we obtain the following:

$$A_e = -10.00 \qquad B_e = +1.000$$
$$A_i = -11.301 \qquad B_i = +1.000$$

Since the in-flight data received can commence at any point in the 1024-sec time sequence between calibrates, these preflight values of A and B are used to process the initial data before the first in-flight calibrate is encountered in each data set.

As shown in Table 1, each amplifier is fed two levels of known, stable input currents once every 1024 sec. On each amplifier these consist of two, 2-sec periods (14 data points each) for each of which an average value of output voltage V is obtained.

Let $V_{1e}$, $V_{2e}$, $V_{1i}$, and $V_{2i}$ be the calibrate output voltage levels for Calibrations 1 and 2 of the electron and ion sensors, respectively. We now obtain updated values for A and B in Eq. (53)

$$A_e = (6\,V_{2e} - 9\,V_{1e})/(V_{1e} - V_{2e}) \tag{54}$$

$$B_e = 3/(V_{1e} - V_{2e}) \tag{55}$$

$$A_i = (7.301\,V_{2i} - 10.301\,V_{1i})/(V_{1i} - V_{2i}) \tag{56}$$

$$B_i = 3/(V_{1i} - V_{2i}) \tag{57}$$

These updated values of A and B are then used for all sensor data in both fixed voltage and sweep voltage modes of operation until the next calibrate is evaluated.
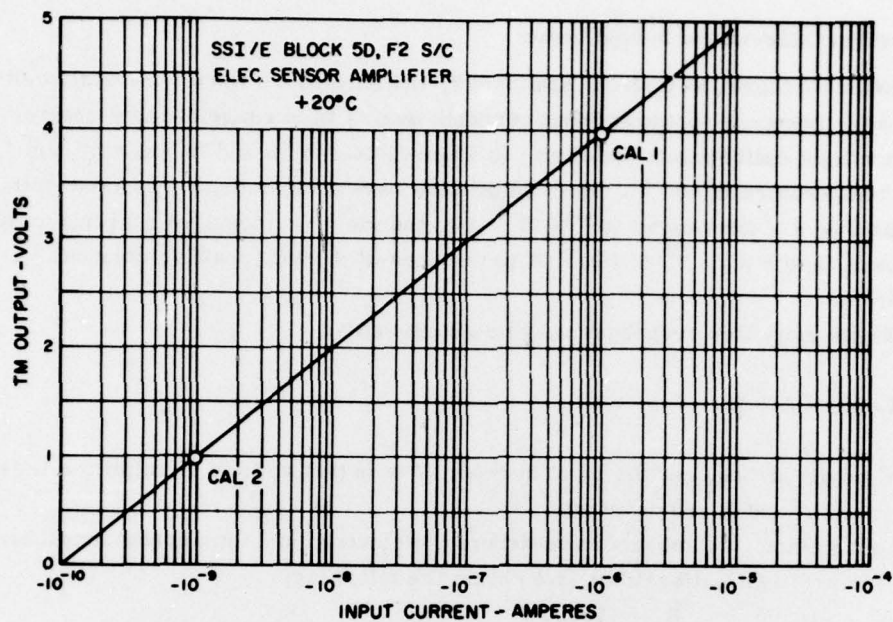
33

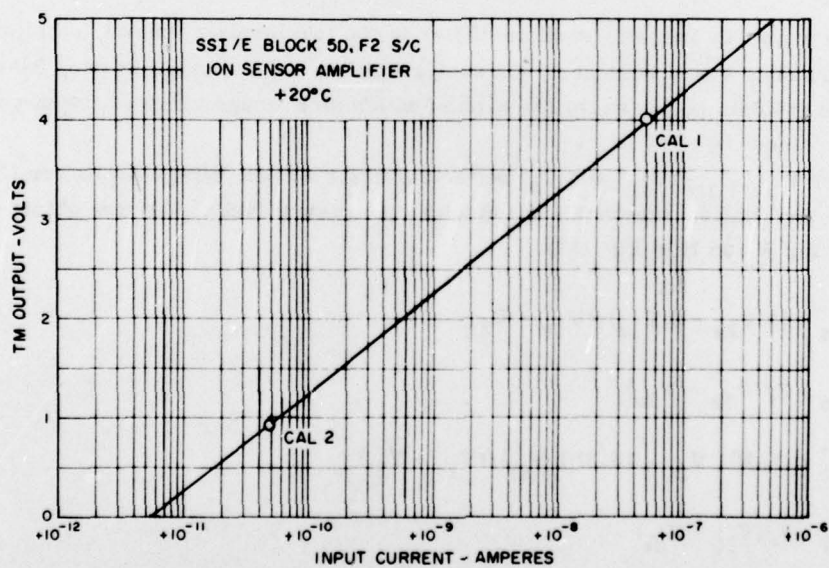Figure 14.   Electron Amplifier Laboratory Calibration, $+20^{O}C$



Figure 15.   Ion Amplifier Laboratory Calibration, $+20^{O}C$

34

Table 3. Electron Sensor Amplifier Laboratory Calibration, $+20^{\circ}C$, Block 5D, F2

Calibration 1 ($10^{-6}$ A): $+3.964$ V
Calibration 2 ($10^{-9}$ A): $+0.978$ V

Monitor Levels: Electron Sweep $+5$ V $\rightarrow$ $+1$ V
                Sweep Flag       $+0.6$ V
                Calibration 1    $+0.2$ V
                Calibration 2    $+0.4$ V

| -I | $10^{-10}$ | $10^{-9}$ | $10^{-8}$ | $10^{-7}$ | $10^{-6}$ | $10^{-5}$ |
|----|------------|-----------|-----------|-----------|-----------|-----------|
| 1 | -.002 | .975 | 1.972 | 2.968 | 3.964 | 4.963 |
| 2 | .281 | 1.275 | 2.270 | 3.268 | 4.265 | 5.262 |
| 3 | .456 | 1.451 | 2.447 | 3.444 | 4.441 | |
| 4 | .582 | 1.576 | 2.572 | 3.568 | 4.566 | |
| 5 | .680 | 1.673 | 2.669 | 3.665 | 4.662 | |
| 6 | .758 | 1.752 | 2.748 | 3.744 | 4.741 | |
| 7 | .826 | 1.819 | 2.815 | 3.811 | 4.808 | |
| 8 | .885 | 1.877 | 2.872 | 3.868 | 4.866 | |
| 9 | .934 | 1.928 | 2.923 | 3.919 | 4.917 | |
| 10 | .980 | 1.974 | 2.969 | 3.965 | 4.963 | |

Table 4. Ion Sensor Amplifier Laboratory Calibration, $+20^{\circ}$C, Block 5D, F2

Calibration 1 $(5 \times 10^{-8}$ A): $+3.984$ V
Calibration 2 $(5 \times 10^{-11}$ A): $+0.976$ V

Monitor Levels: Ion Sweep $\quad +1$ V $\rightarrow$ $+5$ V
Sweep Flag $\quad +0.8$ V
Calibration 1 $\quad +0.2$ V
Calibration 2 $\quad +0.4$ V

| +I | $10^{-12}$ | $10^{-11}$ | $10^{-10}$ | $10^{-9}$ | $10^{-8}$ | $10^{-7}$ |
|----|------------|------------|------------|-----------|-----------|-----------|
| 1  |            | .256       | 1.275      | 2.285     | 3.285     | 4.282     |
| 2  |            | .557       | 1.580      | 2.587     | 3.585     | 4.582     |
| 3  |            | .740       | 1.759      | 2.763     | 3.761     | 4.757     |
| 4  |            | .865       | 1.883      | 2.888     | 3.885     | 4.881     |
| 5  | .025       | .967       | 1.983      | 2.986     | 3.982     | 4.976     |
| 6  | .067       | 1.046      | 2.063      | 3.065     | 4.060     | 5.055     |
| 7  | .121       | 1.119      | 2.132      | 3.132     | 4.127     |           |
| 8  | .166       | 1.170      | 2.188      | 3.189     | 4.185     |           |
| 9  | .221       | 1.227      | 2.241      | 3.240     | 4.236     |           |
| 10 | .260       | 1.271      | 2.287      | 3.286     | 4.282     |           |